Utah State University
DigitalCommons@USU

Space Dynamics Lab Publications | Space Dynamics Lab

1-1-1995

Sensitivity Model for the Wide-Field Infrared Explorer Mission

John C. Kemp
Utah State University

Roy W. Esplin
Utah State University

Perry B. Hacking

Follow this and additional works at: https://digitalcommons.usu.edu/sdl_pubs

Recommended Citation

Kemp, John C.; Esplin, Roy W.; and Hacking, Perry B., "Sensitivity Model for the Wide-Field Infrared Explorer Mission" (1995). *Space Dynamics Lab Publications.* Paper 67.
https://digitalcommons.usu.edu/sdl_pubs/67

This Article is brought to you for free and open access by the Space Dynamics Lab at DigitalCommons@USU. It has been accepted for inclusion in Space Dynamics Lab Publications by an authorized administrator of DigitalCommons@USU. For more information, please contact digitalcommons@usu.edu.

Invited Paper
Kemp, John C., Roy W. Esplin, and Perry B. Hacking. 1995. "Sensitivity Model for the Wide-Field Infrared Explorer Mission." *Proceedings of SPIE* 2553: 26–37. doi:10.1117/12.221359.

Sensitivity model for the wide-field infrared explorer mission

John C. Kemp, Roy W. Esplin

Space Dynamics Lab, Utah State University
1695 North Research Park Way, Logan, Utah 84341-1942

and

Perry B. Hacking

Jamieson Science and Engineering
Suite 505W, 7315 Wisconsin Avenue
Bethesda, Maryland 20814

ABSTRACT

The Wide-Field Infrared Explorer (WIRE) is a cryogenically cooled infrared telescope being prepared to study the evolution of starburst galaxies. The WIRE instrument will measure the infrared energy in two broad bands. Two 128- x 128-pixel arsenic-doped silicon focal plane arrays detect the galatic emissions. We provide a sensitivity analysis for the long wavelength band, 21 to 27 μm, including NEP for a single element. Ultimate flux sensitivity is limited by imaging resolution which includes the effects of diffraction, spacecraft jitter, and sampling of the point spread function. Observation times to obtain these confusion limited measurements are provided. Ground characterization and on-orbit calibration measurements are outlined, as is the simulation plan.

Keywords: infrared astronomy, small explorer missions, sensitivity analysis, confusion limited survey, on-orbit calibration, non-uniformity correction

1. INTRODUCTION

The Wide Field Infrared Explorer (WIRE) is a cryogenically cooled infrared telescope being prepared to study distant galaxies by the Jet Propulsion Laboratory (JPL) teamed with the Space Dynamics Laboratory (SDL). This experiment, one of the NASA Small Explorer Missions, is scheduled for launch in October of 1998. It will be lifted in a spacecraft bus provided by Goddard Space Flight Center to a 500 km sun-synchronous orbit by a Pegasus XL. The WIRE instrument will conduct two different surveys of galaxies with unusually high star formation rates, or "starburst" galaxies. These starburst galaxies are important because, although they comprise only ten percent of the local galaxy population, they represent 30 percent of the local universe energy budget. If they have undergone evolution since formation, they may represent the main source of stars in the universe today. The expected results of the two WIRE surveys will be a catalog of over 30,000 starburst galaxies which will yield insight to their evolutionary history out to redshifts of 0.5-1.0. Extremely luminous galaxies may be detected beyond redshifts of 5. The WIRE objective is to answer the following three questions: (1) What fraction of the luminosity of the universe at a redshift of 0.5 and beyond is due to starburst galaxies? (2) How fast and in what ways are starburst galaxies evolving? (3) Are luminous protogalaxies common at redshifts less than 3?

The WIRE instrument is enclosed in a solid-hydrogen-cooled cryostat, which is described by Batty, et al., 1994.[1] A cassegrain telescope with diamond-turned mirrors provides a light-weight optical system for photon collection., Figure 1 is a sectional view of this telescope. Discrimination between the two broad spectral bands (9-15 μm and 21 to 27 μm) is provided by a dichroic, aided in the short wavelength band by a band-pass filter. Detection and conversion of the photons to electrons is provided by two each 128- x 128-pixel Si:As Impurity Band Conduction Focal Plane Arrays (IBC FPAs) cooled to 7.5 Kelvin. These arrays feature exceptionally low dark current and low read noise, which allow the coaddition of thousands of images. The WIRE instrument and mission were described in recent papers by Kemp et al.[2], 1994 and Elliot *et al.*, 1994.[3]

 0-8194-1912-5/95/$6.00

Downloaded From: http://proceedings.spiedigitallibrary.org/ on 09/24/2014 Terms of Use: http://spiedl.org/terms

In this paper , we will first determine the noise equivalent power for a single element of the long wavelength focal plane array. We will then tell how this result is influenced by spatial noise arising in the FPA. We will introduce the concept of confusion-noise limited measurements and estimate the exposure time required to achieve this condition. We will then discuss the ground characterization and in-orbit calibration plans before finishing with a discussion of plans for simulating the entire system. The purpose of this work is to allow prediction powers so that we can know how faint, and by implication, how distant the galaxies will be that we can detect. The success of this mission will be based in part on our ability to estimate the sensitivity of the WIRE instrument and to incorporate it into the WIRE survey strategy and planning.

2. NEP CALCULATION

As a beginning point we calculate the expected noise performance of a single pixel, assuming that it will be representative of the performance of the array as a whole. Single element detectors are often characterized by parameters such as Noise Equivalent Power (NEP). To calculate NEP we begin by finding the flux Q_{BA} on the detector, made up of the sum of the flux Q_B from the telescope at 17K and the flux Q_A from the astronomical background, consisting of contributions from the zodical scattering from the sun, the zodical emission, and the galactic emission. The astronomical photoelectron background has been determined to be

$$Q_A = 1.612 \cdot 10^9 \cdot \text{electrons} \cdot \text{cm}^{-2} \cdot \text{sr}^{-1} \cdot \text{sec}^{-1}$$

The photocurrent per pixel from this background is given by

$$I_{BA} := Q_A \cdot A \cdot \Omega_{pix} \qquad \text{(electrons/sec)} \qquad (1)$$

where A is the effective area of the telescope, Ω_{pix} is the solid angle field of view of a pixel. If it is assumed that the pixel sees a 17K background with an emissivity of 1 and a 4π steradian field of view the contribution from thermal emission is less than one electron per second, and can be neglected.

$$I_{BA} = 4.818 \cdot 10^3 \cdot \text{electrons} \cdot \text{sec}^{-1}$$

The background noise current is given by

$$I_{BN} := q \cdot \sqrt{2 \cdot I_{BA}} \qquad \text{(Amps/root Hz)} \qquad (2)$$

$$I_{BN} = 1.573 \cdot 10^{-17} \cdot \text{sec}^{-0.5} \cdot \text{coul}$$

The Noise Equivalent Power is given by

$$NEP := h \cdot \frac{c}{\lambda_{avg}} \cdot \frac{I_{BN}}{q \cdot \tau \cdot QE_{avg}} \cdot \text{sec}^{-.5} \qquad NEP = 5.48 \cdot 10^{-18} \cdot \text{Watt} \qquad \text{(BLIP)} \qquad (3)$$

Where the NEP is labeled as BLIP, indicating background limited infrared photodetector, because the performance is limited by the infrared background and not by detector or electronics noise considerations. NEP is not particularly useful to the astronomers who would prefer to see the results expressed in units of Janskys. For those unfamiliar with the unit of Jansky (Jy), this name has been assigned to the flux unit of 10^{-26} Watt meter^{-2} Hertz^{-1}. Hertz is the spectral bandwidth normalization.[4] The NEP number can be converted to equivalent Janskys for the WIRE telescope following the procedure given by Spiro.[4] Note that this result is for a one second exposure in the absence of other noise sources.

$$NEJy := NEP \cdot \frac{\lambda_{avg}^2}{A \cdot (\Delta\lambda) \cdot 3 \cdot 10^{-18}} \cdot \text{Jy} \cdot \text{kg}^{-1} \cdot \text{m}^{-1} \cdot \text{sec}^3 \qquad NEJy = 2.953 \cdot \text{mJy} \qquad (4)$$

7/10/95 11:35:20 PM WSENSIT7.MCD 6

Downloaded From: http://proceedings.spiedigitallibrary.org/ on 09/24/2014 Terms of Use: http://spiedl.org/terms

We next consider the effects of the detector dark current and the associated read noise The total current is given by the sum of the background current I_{BA}, the dark current I_{dk}, and the read noise R_e.

$$I_T := I_{BA} + I_{dk} + \frac{R_e^2}{T_R} \qquad I_T = 5.793 \cdot 10^3 \cdot \text{electrons} \cdot \text{sec}^{-1} \tag{5}$$

Where T_R is the integration time, or the time between detector reads. Note that the read noise only occurs when a pixel is read, and the effective current contributed by it decays with time.

The associated noise current, given in terms of electrons per root Hertz I_{TNe}, and in terms of Amps per root Hertz I_{TN}, are given by

$$I_{TNe} := \sqrt{2 \cdot I_T} \qquad I_{TNe} = 107.638 \cdot \text{electrons} \cdot \text{sec}^{-.5} \tag{6}$$

$$I_{TN} := q \cdot \sqrt{2 \cdot I_T} \qquad I_{TN} = 1.724 \cdot 10^{-17} \cdot \text{sec}^{-0.5} \cdot \text{coul} \tag{7}$$

$$NEP := \frac{h \cdot c}{\lambda_{avg}} \cdot \frac{I_{TN}}{q \cdot \tau \cdot QE_{avg}} \cdot \text{sec}^{-.5} \qquad NEP = 6.008 \cdot 10^{-18} \cdot \text{Watt} \tag{8}$$

Note that the NEP has changed little with the addition of the dark current and read noise. It would be instructive to plot the noise currents asssociated with each of these currents, and that associated with a variable signal irradiance and their sum, see Figure 2. The total noise current is dominated by the natural background until the signal irradiance reaches a level of about 100 photons/sec cm^2 at the telescope aperture.

3. SPATIAL NOISE CONSIDERATIONS

The above calculations would be valid for a single element detector. It would be fantastic if the results for a single pixel could simply be extended to the entire array, but the real world does not work this way. For an imaging array it may be difficult to achieve BLIP performance due to nonuniformities from detector to detector across the array which lead to spatial noise, (often called pattern noise). These responsivity variations can be caused by variations in detector elemental area, small variations in detector element temperatures across the array, and variations in several process control factors which lead to detector quantum efficiency variations, variations in detector spectral response, and differences in coupling to - and gain of - interfacing electronics. These variations can be understood better if we understand that there are often as many as seven individual FET elements in each cell of a source-follower-per-detector readout circuit. Thus, there are many opportunities for minute variations in material properties or lithographic dimensional variations to multiply to the point where they become significant.

Nonuniformity corrections (NUCs) are performed to reduce the effects of these spatial variations, but even this technique does not fully eliminate spatial noise. This after-correction residual spatial noise can be more damaging than temporal noise because it cannot be reduced with time averaging.[5] If the nonuniformities could all be treated as simple variations in individual detector responsivities, and if the responsivities were linear, it would be possible to correct for the nonuniformity and remove the pattern noise using a two-point calibration with an algorithm that corrected each detector for both gain and offset variations.[6] It is possible to use a two-point correction with end points that are very close together to greatly reduce the spatial noise over a limited range of input levels. Or, with more points in the NUC, the spatial noise can reduced close to the level of the temporal noise, but then NUC becomes more complex. "To achieve BLIP performance, the nonlinearity between calibration points should be less than 0.1%".[5] By appropriate flat fielding, we should be able to reduce fixed pattern noise to negligible levels.

However, we must still deal with the issue of drift in the FPAs. Two conditions are generally blamed for drift in detector outputs. System instabilities such as drift in the bias voltages or FPA temperature are one cause. The second cause is 1/f

Downloaded From: http://proceedings.spiedigitallibrary.org/ on 09/24/2014 Terms of Use: http://spiedl.org/terms

noise originating in the individual unit cells of the FPA.[7] System level drift can be addressed by careful design, but the low frequency drift in the individual unit cells is a more difficult problem to solve. Over time, these drifts can be large enough to degrade the system performance below the temporal noise level. These drifts demonstrate a trend proportional to the natural logarithm of the elapsed time since last calibration.[5] Because of this drift, it would be preferable to perform a NUC before each frame of data, but efficiency of measurement would be destroyed. A concept has been suggested to use a scene based correction scheme, where the aperture would not need to be blocked, but each frame could be corrected based on image processing of the preceding set of frames.[7] For the WIRE case this is enabled by fact that data can be processed on the ground after the collection, and the NUC need not be done real time.

WIRE has two built-in stimulator sources to use in uniformly illuminating the focal planes to enable measurement of the flat field response. (These stimulators will be used for pixel-to-pixel response, and not necessarily for global responsivity variations). In addition, the observation pattern will produce data useful for flat fielding by generation of a "supersky" image. In a certain sense it can be said that WIRE is performing spatial averaging. The planned orbital geometry will allow observing the same astronomical field for about 16 minutes during an orbit. The baseline calls for about 15 data frames of 64 seconds each. Between each frame the spacecraft will be dithered in a systematic manner to move the viewing region by about 5 pixels. Each of these 64 second integrations will be recorded. To generate the non-uniformity correction on the ground the median for each pixel will be calculated for the 15 frames and subtracted from each pixel value for each of the data frames. The image is then reconstructed by spatially registering the individual frames and coadding them together. Thus, the measurement at a given sky position combines measurements from 15 different pixels in the array. Since each pixel's median offset, dark current, and background during the 16-minute observing segment has been subtracted, spatial responsivity differences now apply only to the remaining signal (which is dominated by shot noise from the background) instead of the entire background signal. Stimulator flashes which flood the FPA in a uniform and known way taken during the segment can also track small relative responsivity drifts among the pixel elements if necessary.

4. OPTICAL AND SPACECRAFT EFFECTS

The effects considered so far have been detectors characteristics and variability. We next consider the effects of the imperfect optical system collecting photons and focusing them on the FPA. We also consider the fact that the spacecraft attitude control system is imperfect and has a finite jitter in trying to maintain a staring condition during the portion of an orbit assigned to view a particular target spatial region.. The telescope can be characterized by a point spread function given in terms of the full width at half maximum ($FWHM_{tel}$)

$$FWHM_{tel} := \frac{1.04 \cdot \lambda_{avg}}{D_{tel}} \qquad FWHM_{tel} = 16.964 \cdot arcsec \tag{9}$$

For the obstructed system the FWHM is actually less than that given by the equation above but there is less energy in the central lobe, partially compensating for this effect. The rms spacecraft jitter σ_{scj} is specified to be less than or equal to 6 arcseconds. Assuming a Gaussian distribution for this jitter, the full width half maximum number for the spacecraft is

$$FWHM_{sc} := 2.35 \cdot \sigma_{scj} \tag{10}$$

The effective full width half maximum for the total instrument FWHM is calculated assuming both components add in quadrature.

$$FWHM := \sqrt{FWHM_{tel}^2 + FWHM_{sc}^2} \tag{11}$$

$$FWHM = 22.059 \cdot arcsec \qquad FWHM = 106.944 \cdot urad$$

Downloaded From: http://proceedings.spiedigitallibrary.org/ on 09/24/2014 Terms of Use: http://spiedl.org/terms

The number of FPA pixels included within the FWHM is given by the ratio of the FWHM to the angular width of a pixel.

$$\frac{FWHM}{pix_a} = 1.49 \tag{12}$$

The fraction of energy collected by one pixel is given by

$$fr_{pix} := .338$$

where the effects of neighboring pixels have been considered. With this flux spreading due to the telescope blur and the spacecraft jitter, the effective NEP is increased as given by

$$NEP_S := \frac{NEP}{fr_{pix}} \qquad NEP_S = 1.778 \cdot 10^{-17} \cdot Watt \tag{13}$$

5. CONFUSION NOISE CONSIDERATIONS

The WIRE mission will observe faint galaxies. There are large numbers of these very faint galaxies within a single WIRE point spread response function. The rms flux variation from these sources at different positions on the sky is called confusion noise. This effect was first calculated correctly by Scheuer,[8] and applied to the case of a filled aperture by Condon.[9] Condon showed that if the sources being measured are assumed to be unresolved and placed randomly on the sky, the probability distribution of the flux variations is determined entirely by the telescope beam shape and area and the differential form of the source number flux-density relation.[9]

The measurement of the flux density of a point source can be reduced to finding the difference between the peak deflection produced by the source and the background level of the surrounding sky. Background data is often obtained by averaging the data over several beamwidths on either side of the source being measured. Condon showed that "the flux density error distribution for confusion-limited measurements is nearly the same as the confusion deflection distribution P(D) and only slightly broadened by baseline errors". Condon also derived the amplitude distribution of apparent flux densities due to confusion sources observed by a pencil beam telescope.[9] Based upon these results we derived a number of constants applicable to the WIRE instrument.[10]

We estimated the rms confusion Noise for a 232-mm effective telescope and an average wavelength of 24 micrometers, assuming modest galaxy evolution to be

$$\sigma_{c_D232_\lambda 24} := .0508 \cdot mJy$$

The proposed five-sigma, 25μm flux detection limit is given by

$$F_{ps_\lambda 25} := 0.37 \cdot mJy$$

A typical starburst galaxy spectral index for small changes in wavelength is $p := 1.5$

The Signal-to-Noise Ratio for the faintest detectable point source is assumed to be $SNR := 5$

The flux density of the faintest detectable point source as a function of frequency is given by

$$F_{\nu ps}(\nu) := F_{ps_\lambda 25} \cdot \left(\frac{\nu_{\lambda 25}}{\nu}\right)^p \tag{14}$$

Downloaded From: http://proceedings.spiedigitallibrary.org/ on 09/24/2014 Terms of Use: http://spiedl.org/terms

The flux density at the average wavelength is

$$F_{ps_\lambda avg} := F_{\nu ps}(\nu_{\lambda avg}) \qquad F_{ps_\lambda avg} = 0.342 \cdot mJy \tag{15}$$

The photon flux of the faintest detectable point source is

$$E_{ps} := \int_{\nu_1}^{\nu_2} \frac{F_{\nu ps}(\nu)}{h \cdot \nu} \cdot \eta G \tau \left(\frac{c}{\nu}\right) d\nu \qquad E_{ps} = 0.023 \cdot photons \cdot cm^{-2} \cdot sec^{-1} \tag{16}$$

The total allowable rms noise is

$$\sigma_{tot} := \frac{F_{ps_\lambda avg}}{SNR} \qquad \sigma_{tot} = 0.068 \cdot mJy \tag{17}$$

For the confusion noise limited case we need to modify the FWHM to include the pixelation effects , assuming they add in quadrature.

$$FWHMP := \sqrt{FWHM^2 + .5 \cdot (pix_a^2)} \qquad FWHMP = 1.184 \cdot 10^{-4} \tag{18}$$

The effective telescope diameter, which is necessary to scale the confusion noise, is

$$D_{eff} := \frac{D_{tel} \cdot FWHM_{tel}}{FWHMP} \qquad D_{eff} = 208.434 \cdot mm \tag{19}$$

The rms confusion noise at these faint flux levels, for small changes in effective telescope diameter and average wavelength is given by

$$\sigma_{conf} := \sigma_{c_D232_\lambda 24} \cdot \left(\frac{24 \cdot \mu m}{\lambda_{avg}}\right)^{-p} \cdot \left(\frac{232 \cdot mm}{D_{eff}}\right)^{1.6} \qquad \sigma_{conf} = 0.059 \cdot mJy \tag{20}$$

where the 232 mm diameter corresponds to the point spread function assumed in the initial WIRE proposal based upon a perfect optical system and perfect pointing. The maximum allowable instrument noise is given by

$$\sigma_{inst} := \sqrt{\sigma_{tot}^2 - \sigma_{conf}^2} \qquad \sigma_{inst} = 0.034 \cdot mJy \tag{21}$$

This number might be compared with incredulity to the NEJy number computed for a single pixel. We must remember that this tremendous increase in sensitivity comes at the price of very long integration times as we shall see below. Thus, the required instrument signal-to-noise ratio is given by

$$SNR_{inst} := \frac{F_{ps_\lambda avg}}{\sigma_{inst}} \qquad SNR_{inst} = 10.009 \tag{22}$$

5.1 Detector photoelectron flux

From a point source at the flux limit $\Phi_{ps} := E_{ps} \cdot A \cdot fr_{pix}$ $\qquad \Phi_{ps} = 4.475 \cdot electrons \cdot sec^{-1}$ (23)

Downloaded From: http://proceedings.spiedigitallibrary.org/ on 09/24/2014 Terms of Use: http://spiedl.org/terms

From the background

$$\Phi_{bk} := L_{bk} \cdot A \cdot \Omega_{pix} \qquad \Phi_{bk} = 4.818 \cdot 10^{3} \cdot \text{electrons} \cdot \text{sec}^{-1} \tag{24}$$

5.2 Required exposure time

The required explosure time to reach the flux limit is given by

$$T := \left(\frac{SNR_{inst}}{\Phi_{ps}}\right)^{2} \cdot \left(\Phi_{ps} + \Phi_{bk} + I_{dk} + \frac{R_e^{2}}{T_R}\right) \qquad T = 2.9 \cdot 10^{4} \cdot \text{sec} \qquad T = 8.057 \cdot \text{hr} \tag{25}$$

The number of reads per exposure time $N_R := \frac{T}{T_R}$ $\qquad N_R = 7.251 \cdot 10^{3}$ (26)

5.3 Noise terms in electrons

The rms value of each noise term is:

Noise due to signal

$$\sqrt{\Phi_{ps} \cdot T} = 360.255 \cdot \text{electrons} \tag{27}$$

Noise due to background

$$\sqrt{\Phi_{bk} \cdot T} = 1.182 \cdot 10^{4} \cdot \text{electrons} \tag{28}$$

Noise due to dark current

$$\sqrt{I_{dk} \cdot T} = 3.186 \cdot 10^{3} \cdot \text{electrons} \tag{29}$$

Noise due to read noise

$$\sqrt{N_R \cdot R_e^{2}} = 4.258 \cdot 10^{3} \cdot \text{electrons} \tag{30}$$

The total rms noise is

$$\sqrt{\Phi_{ps} \cdot T + \Phi_{bk} \cdot T + I_{dk} \cdot T + N_R \cdot R_e^{2}} = 1.297 \cdot 10^{4} \cdot \text{electrons} \tag{31}$$

5.4 Other time values

The maximum time between reads (Time it takes to fill well)

$$T_{RMAX} := \frac{N_{wc}}{\Phi_{bk} + \Phi_{ps} + I_{dk}} \qquad T_{RMAX} = 48.152 \cdot \text{sec} \tag{32}$$

This time is defined as the time at which the noise from the background equals all other noise sources

$$T_{RBK} := \frac{R_e^{2}}{\Phi_{bk} - I_{dk} - \Phi_{ps}} \qquad T_{RBK} = 0.56 \cdot \text{sec} \tag{33}$$

Downloaded From: http://proceedings.spiedigitallibrary.org/ on 09/24/2014 Terms of Use: http://spiedl.org/terms

6. CHARACTERIZATION AND CALIBRATION

6.1 Ground characterization

Careful ground characterization and on-orbit calibration are crucial to verify that the WIRE instrument will be able to make the desired galactic measurements. Ground characterization will actually begin during FPA and optical component fabrication with component tests at the vendor's facilities. Integrated instrument characterization will be performed at SDL using specialized calibration equipment which is mated to the WIRE sensor with integral vacuum space and contiguous cold shields to preserve the required cold background conditions.

There are three categories of characterization tests which will be done on the ground. The first category includes measurements which are required to be done on the ground because they cannot be duplicated in space. There are three measurements in this category: filter transmission verses wavelength, detector response verses wavelength, and dark current verses bias and temperature. It is possible that the two spectral response measurements can be done as an early verification at the component level, using process evaluation chips (PEC chips) for the FPA, or witness filters for the dichroic and bandpass filter. It may be difficult to perform these tests at the desired low background level.

The WIRE flight operations team will have the capability of changing the FPA biases over a range of zero to 4 Volts. Based upon FPA characterization, a default level (probably in the range of 1.5 to 2.5 Volts) will be predetermined, but flexibility is maintained to allow variation from this level in case of unexpected conditions. Therefore, the FPA performance will be measured under expected flux level inputs over the range of possible bias conditions. By flowing liquid helium through the cryostat and using heaters at the FPA thermal sinks, we will achieve operation at temperatures different than planned for and enable performance of the bias/operating characterization at a series of different temperatures.

Performance verification constitutes the second major category of ground characterization measurements. The following are under this classification: FPA read noise, response to known input flux levels, signal-to-noise ratios, flux linearity verses temperature and bias. To some extent, these measurements can also be made in orbit, and they will be remeasured during flight; but ground characterization will give an early indication of any sensitivity issues or out-of-specification performance. It will definitely be much easier to perform these measurements during the ground characterization because of both the ease of controlling the input flux in a rapid fashion and also the ability to vary temperature in a controlled fashion. Also, with the availability of ground support equipment with immediate access to the data it will be easier to go back and repeat any data sets that might be questionable or incomplete. As part of this characterization category, a set of qualifying measurements has already been started to quantify the response and recovery to environmental radiation inputs

The third major category of ground characterization deals with ancillary data such as pixel offsets, responsivity, detector linearity, point spread function, stimulator uniformity, array registration and preamp gain and linearity. These data can all be determined just as well in orbit, but an early "heads-up" will be valuable to the program. It is noted that these parameters are expected to change on orbit.

6.2 In-orbit calibration

Once the basic spacecraft and instrument functionality have been reaffirmed after launch, the first 20 days of orbit are assigned to an in-depth in-orbit checkout (IOC) and calibration. (Calibrations will continue on an as-needed basis at intervals determined by the stability indicated during the IOC to accommodate any changing conditions during the duration of the flight.) During this time pixel offsets will be determined by recording and analyzing the response to both zero bias conditions and linearity sequences. Linearity sequences can be achieved by looking at various celestial sources and also by using multiple stimulator flashes. Flat Fielding measurements will also be made using stimulator flashes as well as the "supersky" concept described under "spatial noise".

Also during IOC, a celestial point source will be used to flux calibrate and measure the response and PSF across the array. Gain settings will be cross calibrated. Sets of calibrators at different flux levels and gains will be measured for dynamic range information.. Field distortions and pixel cross-talk will be measured.

Downloaded From: http://proceedings.spiedigitallibrary.org/ on 09/24/2014 Terms of Use: http://spiedl.org/terms

There are a number of constraints to on orbit calibration. The minimum background is expected to be about 4050 photoelectrons per second per pixel . The minimum integration time of .5 seconds sets an upper limit on the flux of the celestial sources to be observed. The maximum flux that can be measured at a .5 second integration time is about 30 Jy. Both Uranus and Neptune are brighter than this level. Asteroids are poor calibration sources because of their variability. Galaxies from the IRAS faint source catalog are possibilities, as are any unconfused, non-variable, small sources less than about 10 Jy, preferably less than 1 Jy, that have been calibrated by previous missions. It is planned to utilize calibrators from the ISO and SPIRIT III missions where possible.

Calibrated data is defined as data which has been linearized, flattened, and converted to flux density units (Janskys) for point sources, with all electrical signatures removed. The necessary steps include removal of offset, dark current, and background levels; removal or replacement of bad pixels, linearization and flat fielding of all remaining data. This is followed by conversion to flux density units based on observation of celestial calibration sources.

7. SIMULATIONS

To verify that critical issues have not been neglected or misinterpreted in these sensitivity calculations, the WIRE program is simulating the data collection/reduction process. Source count distributions are generated for various galaxy evolution scenarios. These distributions and a simulated point spread function (PSF) are used to form "truthimages" that are about 47 by 47 arc minutes in extent, 50 percent larger than needed for the complete field of view of a FPA. The resolution in these truthimages is 1920 by 1920 pixels, ten times finer than the WIRE telescope. The truthimages are then used as the basis for a sequence of coarser images to which noise and other sensor characteristics are added and which can be generated quite quickly.

The point spread function (PSF) is generated at high resolution (5x truthimage resolution) and calculated to a radius of about 300 arcsec. The PSF is modeled as the diffraction pattern of WIRE's circular aperture with central obscuration convolved with a 2-dimensional Gaussian function that simulates spacecraft jitter. The diffraction pattern is calculated at small wavelength increments through the passband and averaged using a weighting factor of $\lambda^{1.5}$, corresponding to the expected energy distribution of the sources of interest, to obtain a composite diffraction PSF for the entire passband. Spider diffraction and aberrations are currently not included in the PSF calculation but these are not expected to be dominant effects. The optical system is expected to be diffraction-limited; however, the PSF has a significant contribution from spacecraft jitter (6 arcsec rms).

A sample of about one million source fluxes is randomly drawn from the appropriate number counts distribution using a lookup table method. A scaled and shifted copy of the PSF is then placed in the truthimage for each of the source fluxes. This produces an average of 30 point sources per WIRE pixel which adequately simulates confusion effects. The sources are placed in uniformly random positions which are saved in a source list for comparison to the reduced data. Once the truthimage is created, a sequence of coordinates is generated indicating nominal positions, actual positions, and errors in the position of the optical axis for each WIRE image to be produced. A "drift error" is simulated that varies from orbit to orbit. A "dither error" is a random pointing error added to each frame.

When the image sequence is generated from the truthimage, a uniform background radiance is assumed at a level comparable to the calculated background level. Radiance is converted to electrons taking quantum efficiency and integration time into account and the simulated dark current is added. For each WIRE image to be generated, a 128x128 reduced-resolution section of the truthimage is extracted. The reduced resolution images are created by summing the 10x10 blocks that most closely match the position of the WIRE pixels (no rotation about the optical axis is simulated). This operation requires significant computation, therefore the WIRE-sampled images are generated in groups that require the same phase of resolution reduction.

The extracted 128x128 image represents the signal flux passing through the FPA surface. For each pixel, the signal flux is converted to units of electrons and summed with the background electrons. A random Gaussian number is then generated using the square-root of this quantity as the standard deviation. The random number, which simulates the Poisson-

Downloaded From: http://proceedings.spiedigitallibrary.org/ on 09/24/2014 Terms of Use: http://spiedl.org/terms

distributed photon noise, is added to the pixel value. A Gaussian noise is further added to simulate the electronic noise. The resulting number is quantized to A/D counts and the resulting 16-bit integer array is written to a file with a header specifying nominal orientation and simulated responsivity. Perfect uniformity of FPA dark current and responsivity is currently assumed; these will be simulated more realistically soon.

This data will then be reduced using the same software that will be used for the flight data reduction; preliminary reductions have already occurred. The resultant data will be analyzed to determine whether the instrument has achieved the desired sensitivity, and if not the source of the discrepancy will be discovered and corrected. The fidelity of the simulation will be improved as the program progresses. This process is already underway to make sure that the WIRE instrument is not built to a non-optimum set of specifications.

8. USE OF THE MODEL

Once the model is available it can be used to predict instrument performance as various parameters are changed. For example, it may be possible to obtain higher performance from the spacecraft attitude control system (ACS), i.e., reduce the spacecraft jitter from 6 arcseconds to a lesser value. As this parameter is changed we note the change in required exposure time. If the jitter can be reduced by a factor of only two to a value of 3 arcseconds, the required exposure time to reach the confusion limits specified is reduced by a factor of four. If this improvement in the ACS is possible, then we look at other options to further improve the WIRE instrument capability . For example, once the observation time is reduced by such a large factor we may be able to make certain other instrument changes that would incrementally lengthen the observation time. Increasing the telescope focal length by about 20 % to reduce the angular width of each pixel to better sample the point spread function also drops the background level in each pixel while keeping the signal level about the same and results in an increase in the measurement time to reach the desired flux limit by about 40%. But, the measurement time is still much lower than originally and the instrument performance is improved. The interactions in a mission such as WIRE are complex enough that it requires a model to assess impacts of potential parameter changes.

9. CONCLUSIONS

A model for the sensitivity of the WIRE mission has been developed. This model shows that it is possible to reach confusion-noise limited measurements within a reasonable measurement time, (2.9×10^4 seconds for the long wavelength band). By integrating and coadding to obtain this long measurement time we can increase the sensitivity by about a factor of 50 over the single pixel case integrated for one second. Confusion-noise limited measurements are enabled by the technique of generating a "supersky" image, wherein dithering in between 64-second data collections is used to remove dark current, offset, and background spatial noise. These sensitive measurements aided by the ability to do extensive processing of the data on the ground and to combine multiple data sets. Careful ground characterization and in-orbit calibration will verify the sensitivity model. Simulations are being used to guard against misinterpretations in the modeling.

10. ACKNOWLEDGMENTS

SDL/USU's definition- and bridge-phase work on the WIRE program has been carried out under subcontract 959786 with the California Institute of Technology Jet Propulsion Laboratory under NASA Contract NAS7-918. SDL/USU is the prime instrument contractor. The authors are particularly indebted to Terry Herter of Cornell for useful conversations and much help with sensitivity calculations and to Helene Schember of JPL, the WIRE program manager. Many other individuals have also made significant contributions to the WIRE program. Of particular mention are Glenn Allred, Harry Ames, Dave Elliot, Wally Gibbons, David Henderson, Kris Huber, Scott Schick, Dean Shaffer, David Shupe, and Allan Steed.

Downloaded From: http://proceedings.spiedigitallibrary.org/ on 09/24/2014 Terms of Use: http://spiedl.org/terms

11. REFERENCES

1. Batty, J. C., D. Murray, and S. Schick, "Cryogenic System for Wide-Field Explorer (WIRE)," paper 2227-23, *Cryogenic Optical Systems and Instrument IV*, SPIE Symposium on Optical Engineering in Aerospace Sensing, Orlando, Florida 4-9 April, 1994.
2. Kemp, J. C., H. O. Ames, R. W. Esplin, and G. D. Allred, "Wide-Field Infrared Explorer (WIRE) instrument description; focal planes, optics, and electronics, *Infrared Spaceborne Remote Sensing II*, Marija S. Scholl, Editor., Proc. SPIE 2268, pp. 56-67, (1994).
3. Elliot, D. G., P. Hacking, H. R. Schember, "Engineering design of the Wide-Field Infrared Explorer (WIRE), *Infrared Spaceborne Remote Sensing II*, Marija S. Scholl, Editor, Proc. SPIE 2268, pp. 188-195, (1994).
4. Spiro, Irving J., "The Jansky as a Unit," *Radiometry and Photometry*, Optical Engineering, 16:6, p. SR-152, 1977.
5. Scribner, D. A., M. R. Kruer, K. Sarkady, and J. C. Gridley, "Spatial noise in staring IR focal plane arrays," *Infrared Detectors and Arrays*, Proc. SPIE 930, pp. 56-63, (1988).
6. Milton, A.F., F. R.Barone, and M. R. Kruer, "Influence of nonuniformity on infrared focal plane array performance," Optical Engineering, 24:5, pp. 855-862, (1985).
7. Scribner, D. A., K. A. Sarkady, M. R. Kruer, and C. J. Gridley, "Test and Evaluation of Stability in IR Staring Focal Plane Arrays After Nonuniformity Correction", *Test and Evaluation of Infrared Detectors and Arrays,* Proc. SPIE 1108, pp. 255-264, (1989).
8. Scheuer, P. A. G., "A Statistical Method for Analysing Observation of Faint Radio Stars," Proceedings. of the Cambridge Philosophical Society, 53, pp. 764-773, (1957).
9. Condon, J. J., "Confusion and Flux-Density Error Distributions", The Astrophysical Journal, 188, pp. 279-286, (March 1, 1974).
10. Hacking, Perry B., "WIRE Sensitivity and Confusion Noise Calculations,", Appendix A, Wide-Field Infrared Explorer (WIRE) Proposal for the Small Explorer Missions Program, Section I Investigation and Technical Plan, Jet Propulsion Laboratory, 12 January 1993, pp. A-1 to A-3.

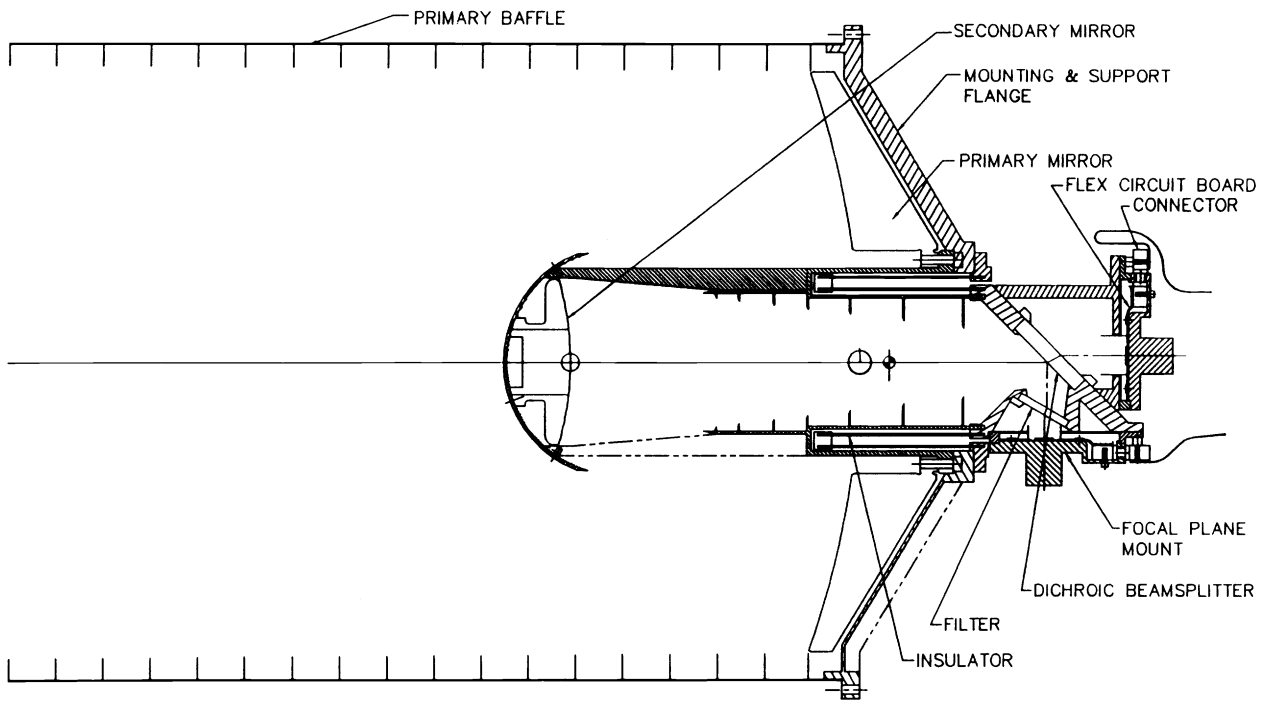

Figure 1. Cross section of WIRE telescope.

Downloaded From: http://proceedings.spiedigitallibrary.org/ on 09/24/2014 Terms of Use: http://spiedl.org/terms

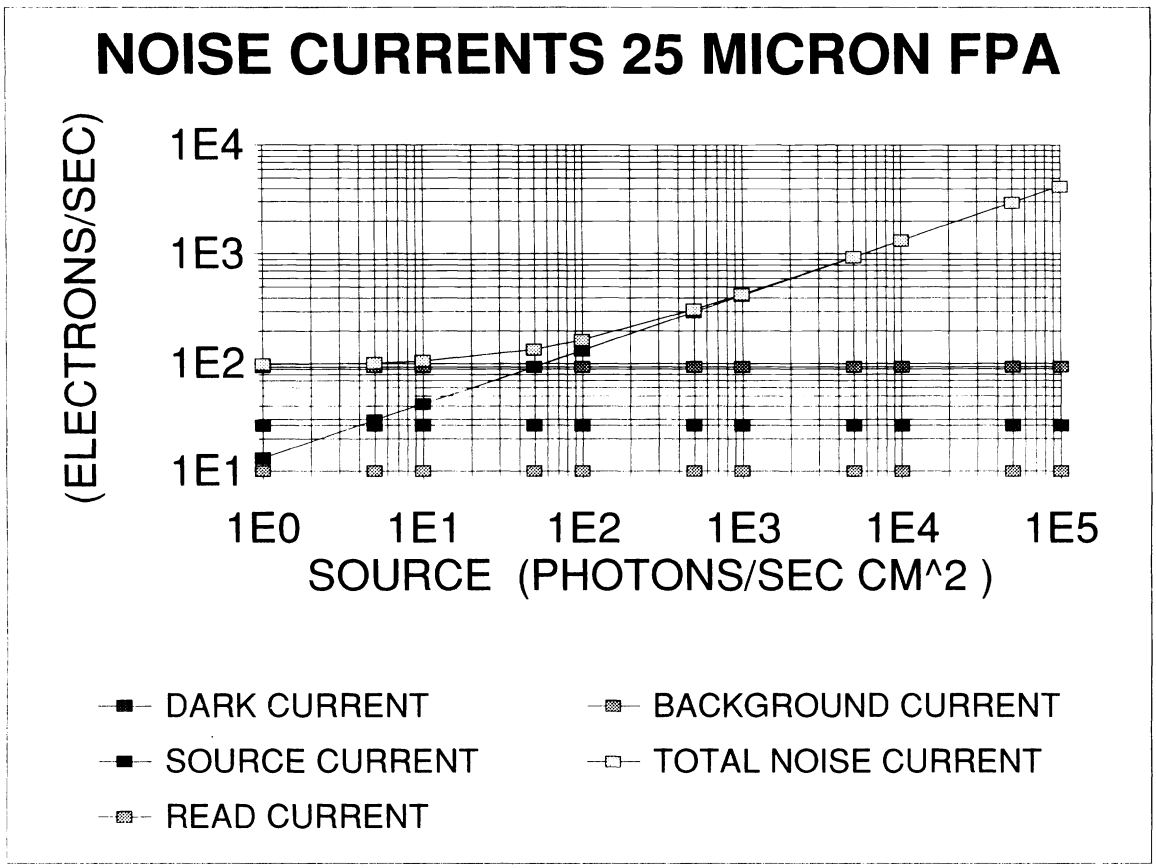

Figure 2. Plot of total noise current and noise currents from various sources for a single pixel for a one second integration time.

Downloaded From: http://proceedings.spiedigitallibrary.org/ on 09/24/2014 Terms of Use: http://spiedl.org/terms